International Journal of Automotive Technology, Vol. 8, No. 5, pp. 533–542 (2007)

1229-9138/2007/036-01

EXPERIMENTAL INVESTIGATION ON THE EFFECT OF MAGNETIC FLUX TO REDUCE EMISSIONS AND IMPROVE COMBUSTION PERFORMANCE IN A TWO-STROKE, CATALYTIC-COATED, SPARK-IGNITION ENGINE

P. GOVINDASAMY[1)*] and S. DHANDAPANI[2)]

[1)]Kongu Engineering College, Erode 638 052, India
[2)]Coimbatore Institute of Technology, Coimbatore 641 014, India

(Received 14 August 2006; Revised 1 August 2007)

ABSTRACT–The two stroke spark ignition engine is the greatest contributor of the total vehicular pollution in a country like India. It is therefore an item that requires great attention in order to reduce fuel consumption and its concomitant pollution. The use of strong magnetic charge in the fuel line gives a complete and clean burn so that power is increased while operating expenses are reduced. The magnetic flux on the fuel line dramatically reduces harmful exhaust emissions while increasing mileage, thereby saving money and improving engine performance. It increases combustion efficiency and provides higher-octane performance. The experimental results show that the magnetic flux on fuel reduces the carbon monoxide emission up to 13% in a base engine, 23% in a copper-coated engine and 29% in a zirconia-coated engine.

KEY WORDS : Energizer, Emission, Spark-ignition engine

1. INTRODUCTION

Transport is the prime source of mobility in urban society. It not only provides a fast, convenient and economical mode of carrier for the multifarious activities of citizens but also caters to the commercial and industrial need for transportation of important goods. However, it vitiates the environment by emanating obnoxious and toxic pollutants and thereby creates serious health hazards to the biotic community.

Automobiles have been castigated as polluters of the environment. Pollution due to automobile emissions is of great concern, particularly in metropolitan cities where it creates a potential threat to the existence of healthy life (Gao and Schreiber, 2002). Thus, safeguarding quality of air from degradation due to transportation is important.

For complete combustion, the air-to-fuel stoichiometric ratio is computed as 14.5 (Kalghahgi, 1986). However, in spark-ignited engines, complete combustion does not take place and pollutants are produced even at stoichiometric values matching this A/F ratio, since the spark-induced reaction is not fully propagated inside the piston chamber.

This paper aims to develop an eco-friendly system to reduce harmful emissions while increasing engine performance. The fuel is energized by keeping a highgauss magnet on the fuel line (Tretyakov *et al.*, 1985). This magnet can be easily installed within minutes by strapping it to the fuel line next to the carburetor.

*Corresponding author. e-mail: pgsamy@kongu.ac.in

2. WORKING PRINCIPLES

2.1. Monopole Technology

The most important factors in the monopole technology are the magnetic field intensity and the collimation (Kronenberg, 1985) of the lines of magnetic flux (Figure 1). Intensity of magnetic field is far superior to that generated by regular permanent magnets; the collimation of magnetic fields renders the lines of magnetic flux exactly parallel to each other at extremely high densities,

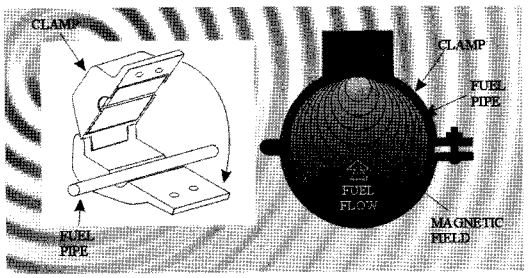

Figure 1. Magnetic fuel energizer.

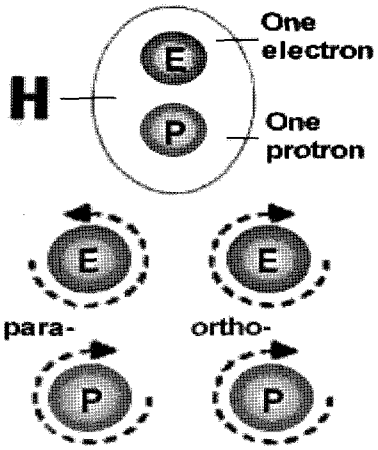

Figure 2. Atomic orientation.

on the order of millions of lines of flux per cm^2. These devices are external online installations which require no cutting or modifying of the fuel pipes.

2.2. Ortho-Para Orientation

In a para-H_2 molecule, which occupies even rotational levels (quantum number), the spin-state of one atom is in the opposite direction relative to another, rendering the molecule diamagnetic. In an ortho molecule, which occupies odd rotational levels, spins are parallel, with the same orientation for the two atoms; this molecule is therefore paramagnetic and may serve as a catalyst for many reactions (Figure 2).

This spin orientation has a pronounced effect on physical properties and behavior of the gas molecule. The coincident spins render *o*-H_2 exceedingly unstable and much more reactive than its *p*-H_2 counterpart. To secure conversion from the *p* to *o* state, it is necessary to change the energy of interaction between spin states of the H_2 molecule (Janczak *et al.*, 1992).

2.3. De-Clustering Fuel

Hydrocarbons basically have a "cage-like" structure. Thus, during the combustion process, oxidation of their inner carbon atoms is hindered. Furthermore, they bind into larger groups of pseudo-compounds, which then form clusters (associations). The access to oxygen in the right quantity for the interior of the molecular groups is hindered; it is this shortage of oxygen to the cluster that hinders full combustion. In order to combust fuel, the proper quantity of oxygen from the air is necessary to oxidize the combustible agents.

The exhaust should theoretically contain carbon dioxide, water vapor and nitrogen from air, which does not participate in the combustion. Practically speaking, the exhaust gases contain CO, H2, HC, NOx and O2. In reality, complete combustion of fuel is never achieved and the incompletely oxidized carbon is evident in the forms of HC, or CO, and is often deposited on the internal combustion chamber walls as black carbon residue. These results are caused by incomplete combustion.

Hydrocarbon fuel molecules treated with the magnetic energy of the mono pole technology tend to de-cluster, creating smaller particles more readily penetrated by oxygen, thus leading to better combustion. They become normalized and independent, distanced from each other, with bigger surfaces available for binding (better attraction) with more oxygen (better oxidation). In accordance with van der Waals' discovery of a weak-clustering force, there is a very strong binding of hydrocarbons with oxygen in such magnetized fuel, which ensures optimal burning of the mixture in the engine chamber

3. THE EXPERIMENTAL SYSTEM

In a single-cylinder, air-cooled, two-stroke SI engine (Table 1), provisions were fabricated and installed in the engine setup to vary ignition timing and fuel quantity. To facilitate operating the engine under maximum-best-torque (MBT) timing mode, a timing gear was designed in such a way that, for one complete rotation of hand wheel, the timing advance/retard measured exactly one degree. By adjusting this hand wheel mechanically, spark timing could be varied at will, even during engine operation.

For a given quantity and quality of the mixture under a given load setting, that timing which gave the maximum torque was taken as the MBT timing. The quantity of fuel was varied by adjusting the fabricated metering rod inserted into the carburetor jet. These two arrangements helped the engine run in MBT operation mode for each load of its operations.

An AVL Electrical Eddy Current dynamometer was coupled to the engine. This provided a facility for controlling speed and load externally by computer and a provision to record speed and torque fluctuations (Figures 3 & 4). An automatic fuel flow meter with digital clock

Table 1. Engine specifications.

Engine make	Bajaj 150 CC
Cylinder bore	57.5 mm
Stroke	58 mm
Displacement	150 cc
Power	4.5 kW @5500 rpm
Con rod length	110 mm
Compression ratio	7.4:1
Carburetor	Jetex, Down draft
Lubrication	Petroil

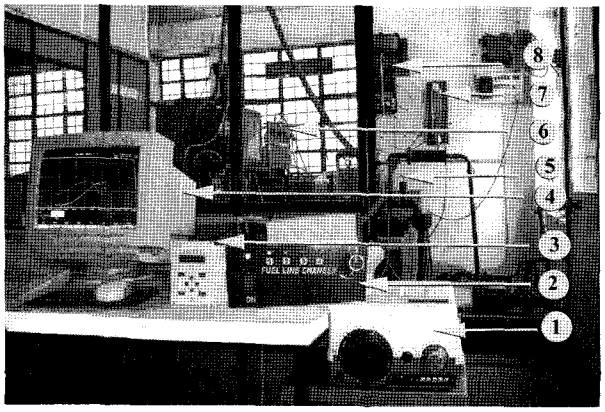

1) Exhaust gas analyzer 2) Fuel line changer 3) Charge amplifier 4) AVL data acquisition system 5) Eddy current dynamometer 6) Fuel line assembly fit 7) Fuel metering unit 8) Fuel recirculation unit

Figure 3. Photographic view of experimental setup.

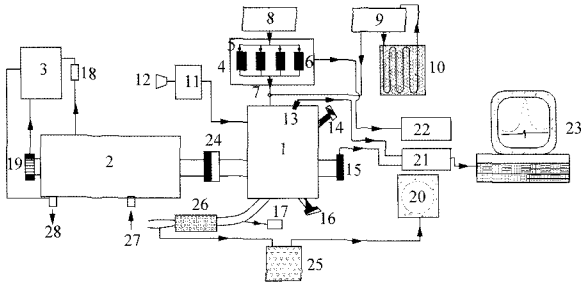

1) Engine 2) Eddy current dynamometer 3) Dynamometer control panel 4) Fuel line assembly kit 5) Solenoid valve 6) High gauss magnet 7) Solenoid valve 8) Primary fuel tank 9) Fuel recirculation tank 10) Radiator core 11) Air box 12) Orifice meter 13) Piezo-electric pressure pickup 14) Variable area jet-screw 15) Crank angle encoder 16) MBT timing gear 17) Exhaust gas temperature sensor 18) Load sensor 19) RPM counter 20) Exhaust gas analyzer 21) Charge amplifier 22) Fuel line changer 23) AVL-data acquisition system 24) Coupling 25) Moisture separator 26) Muffler 27) Cooling water in 28) Cooling water out

Figure 4. Schematic view of experimental setup.

allows accurate fuel flow measurements. Commercially available petrol mixed with propergrade lubricant is used as fuel. A separate fuel tank is maintained beside the main fuel tank. Fuel is drawn from the bottom of the tank by an electronic fuel pump and discharged to the top of the tank. A high-gauss magnet is placed such that north pole faces towards the radiator core surface, which is placed next to the fuel pump. This arrangement is properly shielded to safeguard the data acquisition system. The pump is operated for an hour before the experiment in order to energize the fuel. This fuel recirculation tank can be accessed as one of the fuel resources in the fuel line-changer. The fuel-line assembly kit consists of four fuel lines with solenoid valve controls and LED indicators to show the fuel line is alive.

This kit actually receives fuel either from the main tank or from the recirculation tank, but only from one at a time. All solenoid valves are connected with the fuel-line changer, which is placed adjacent to the on-line data acquisition system. Fuel-line selection can be done in the fuel-line changer itself. The manually adjustable solenoid valve is also fixed for one fuel line for emergency operation. CO and unburnt hydrocarbon emissions are measured by an AVL (Digas 4000 Light) exhaust gas analyzer. Exhaust gases are allowed to pass through a water trap immersed in an ice bath to separate the condensed water, so that only dry exhaust gas is allowed into the exhaust analyzer.

The cylinder pressure was measured using a Kistler-model, piezoelectric pressure transducer flushmounted in the cylinder head of the engine. The output of the transducer was fed to a Kistler model charge amplifier, which possesses a high degree of noise rejection with ground-level current attenuation (Dhandapani, 1991). For each set of readings, pressure data were recorded using a high speed AVL data acquisition system timed by an optical encoder mounted on the engine crankshaft. After collection, each sample was transferred to a hard disk on a personal computer system for storage and further analysis. A sample size of 500 cycles was selected for further analysis. The fuel-line changer with solenoid valves helps to change the fuel line in order to pass fuel in-to a variety of energized banks. This magnetic source magnetizes the fuel coming through the fuel line and better prepares it for combustion (Figure 5).

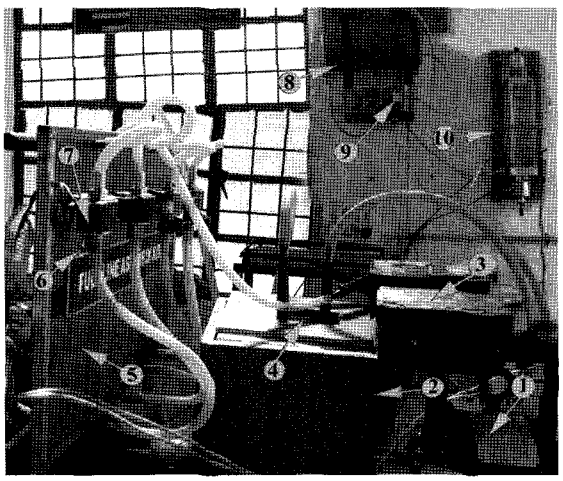

1) Eddy current dynamometer 2) Monopole fuel energizer 3) 4500-Gauss bar magnet 4) Radiator core inside 5) Fuel-line assembly kit 6) Fuel-line indicator (LED) 7) Solenoid valve 8) Fuel recirculation tank 9) Electronic fuel pump 10) Electronic fuel consumption meter

Figure 5. Fuel energizer and fuel line assembly kit.

Initially, the non-magnetized fuel line is selected in the fuel-line changer and the engine is allowed to warm up for 20 min before readings are taken. The engine is operated at a constant speed mode of 3000 rpm, which represents the average cruising road speed of the vehicle.

The exhaust gas analyzer is switched on quite early so that it stabilizes before the experiment begins. Ambient pressure, humidity and temperature are noted. The fuel flow is varied to supply rich and lean mixtures. Ignition timing is kept advanced to run the engine on MBT operation mode. The load on the engine is automatically controlled by the dynamometer while keeping the engine at constant speed.

After the engine is stabilized for a particular operating point, airflow, fuel flow, and exhaust gas temperature are recorded. The dynamometer readings such as load and speed are also noted. At each operating point, cylinder pressure traces of 500 cycles and their average are measured and stored on a computer hard disc (Nedunchezhian and Dhandapani, 1999).

4. MATERIALS USED

Neodymium-Iron-Boron-based magnets (3000 gauss) are used for initial testing purposes. Rare-earth-based magnets (4500 & 9000 gauss) have also been used for testing (Figure 6). The-higher gauss magnets need to be shielded to safeguard the encoder, data acquisition system and dynamometer. A commercially available radiator core was used as a base to keep magnets on both sides and allow fuel to recirculate around the magnets to get energized fuel.

5. METHODOLOGY

The engine was operated at a constant speed mode and

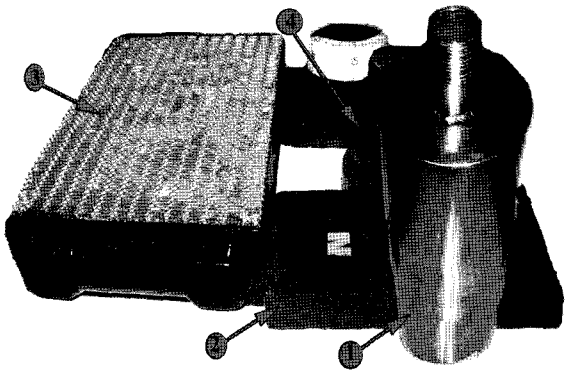

1) 9000-Gauss magnet 2) 4500-Gauss magnet 3) Radiator core 4) 3000-Gauss magnet

Figure 6. Photographic view of different gauss magnets.

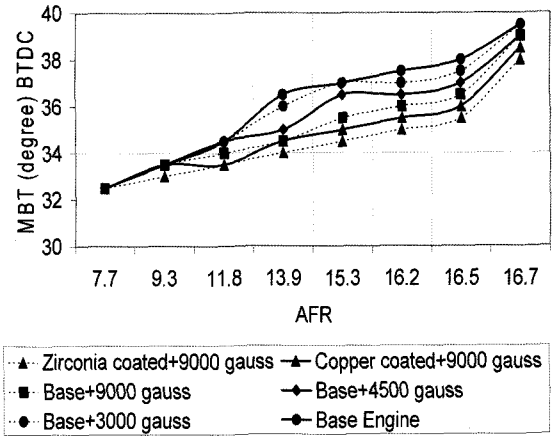

Figure 7. Optimizied MBT for different operating mode.

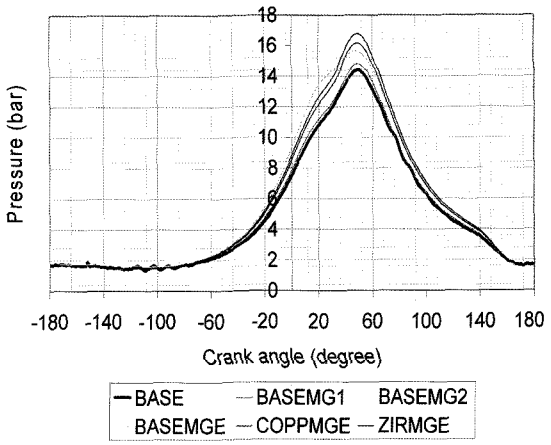

Figure 8. Variation of pressure with crank angle at AFR=9.3.

the following cases were considered: 1) base engine without magnet; 2) base engine with 3000-gauss magnet 3) base engine with 4500-gauss magnet 4) base engine with 9000-gauss magnet 5) copper-coated engine with 9000-gauss magnet and 6) zirconia-coated engine with 9000-gauss magnet. The engine was allowed to run on a lean limit with the help of the fabricated metering rod. MBT was also maintained with the help of a timing gear wheel to validate the experimental data (Figures 7 to 14) with base performance data.

The inner surface of the cylinder head was coated with copper chromate and zirconia by thermal evaporation in a vacuum-coating unit (Figure 15). The above experimental procedure has been repeated and the data collected. Air and fuel are subject to the lines of forces from permanent magnets mounted on the air and fuel inlet lines. The magnet is oriented so that its south pole is located adjacent the fuel line and its north pole is spaced apart from the fuel line.

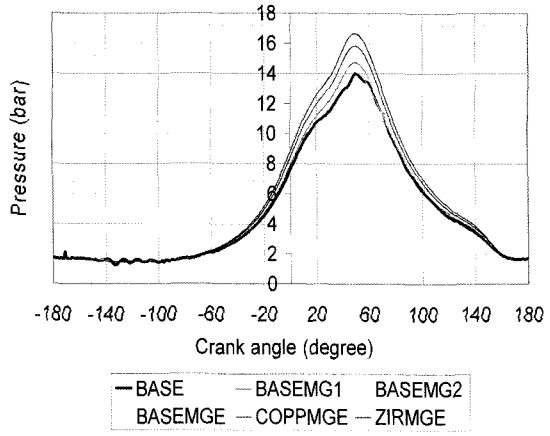

Figure 9. Variation of pressure with crank angle at AFR=11.8.

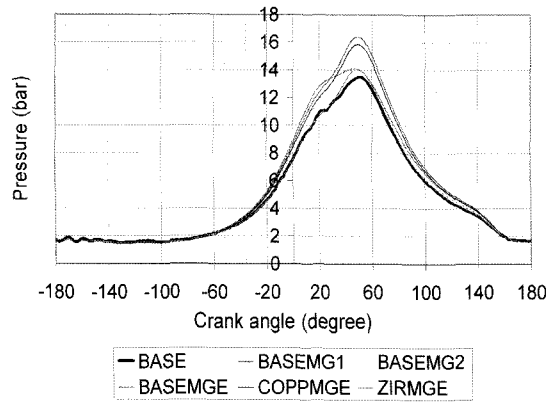

Figure 10. Variation of pressure with crank angle at AFR=13.9.

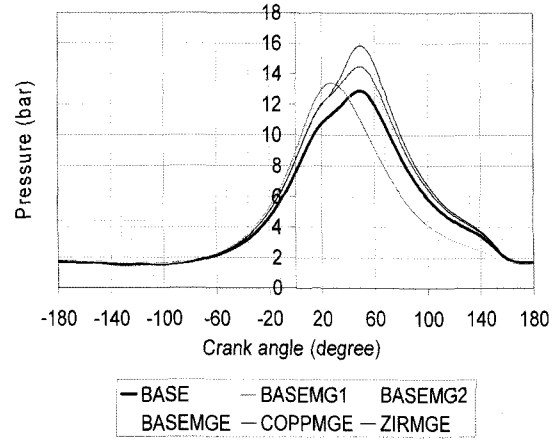

Figure 11. Variation of pressure with crank angle at AFR=15.3.

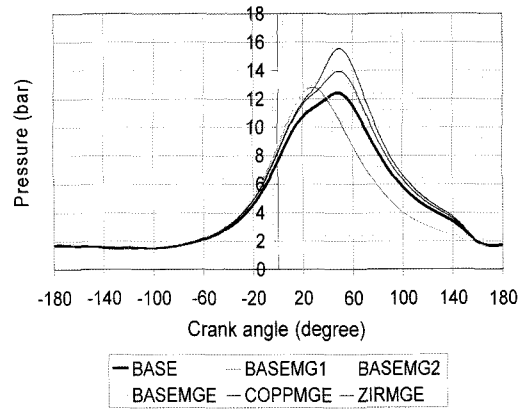

Figure 12. Variation of pressure with crank angle at AFR=16.2.

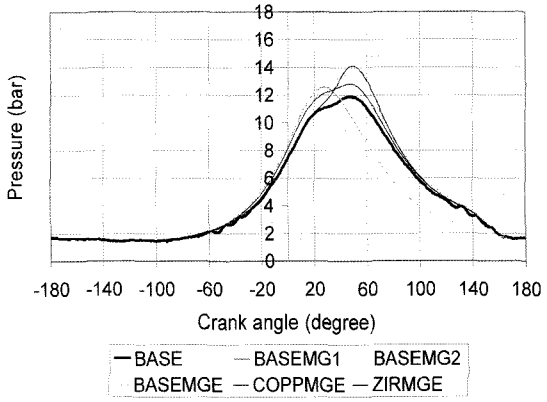

Figure 13. Variation of pressure with crank angle at AFR=16.5.

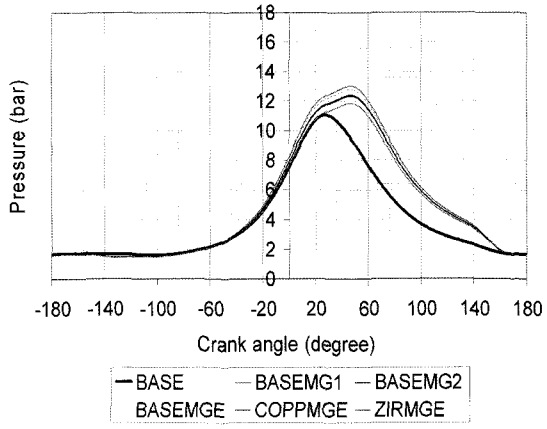

Figure 14. Variation of pressure with crank angle at AFR=16.7.

BASE : Base Engine
BASEMG1 : Base+3000 gauss
BASEMG2 : Base+4500 gauss
BASEMGE : Base+9000 gauss
COPPMGE : Copper coated+9000 gauss
ZIRMGE : Zirconia coated +9000 gauss

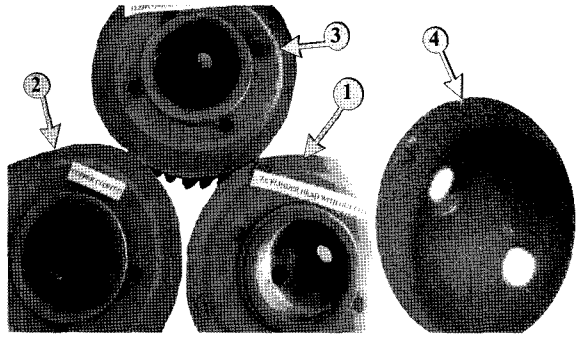

1) Base engine cylinder head 2) Copper-coated cylinder head 3) Zirconia-coated cylinder head 4) Close view of zirconia coating

Figure 15. Photographic view of catalytic coated cylinder heads.

6. RESULTS AND DISCUSSION

6.1. Engine Performance

For the same amount of air-fuel mixture supplied to the engines, the base engine gives a lesser brake power (BP) and brake thermal efficiency (BTE) compared to the energized fuel engine. The same trend is maintained between the base engine and the catalytic-coated engine, with and without energized fuel. This is due to the incomplete combustion of the charge due to the mixture limit inside the combustion chamber at a given compression ratio. The actual volume of charge combusted is comparatively less than the volume of charge entering the chamber. Hence, the amount of fuel charge to give mechanical power is reduced, which in turn reduces the BTE (Figure 16).

Fuel molecules start diffusing from the free stream into the boundary layer; this fuel concentration at various sub-layers and at various crank angle positions is found to be different. The fuel level in the sub-layer near the free stream shows a sudden increase near the TDC because the boundary layer thickness suddenly decreases near the TDC due to the effect of the high Reynolds number. As a result, the effective distance that the fuel molecule diffuses decreases near the TDC, and thus the fuel levels in the sub-layers were higher. The variation in fuel concentration in sub-layers near the wall was less than in the sub-layers near the free stream. This shows that the diffusion rate of fuel is the main controlling factor in limiting the reaction rate. In the magnet (9000 gauss) fuel line, diffusion from the free stream to the layers is found to be greater; hence, maximum charge mass is combusted for a given actual charge. This leads to a higher mechanical power and a higher BTE (Figure 16).

The air-fuel ratio (AFR) for BTE (Figure 16), IMEP (Figure 17), BMEP (Figure 18), Pmax (Figure 19), BSFC (Figure 20), CO (Figure 21) and HC (Figure 22) were

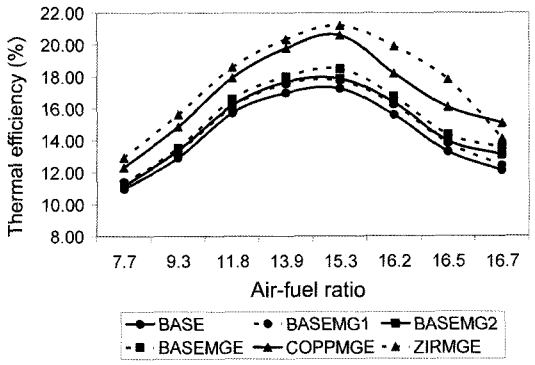

Figure 16. Variation of brake thermal efficiency with air-fuel ratio.

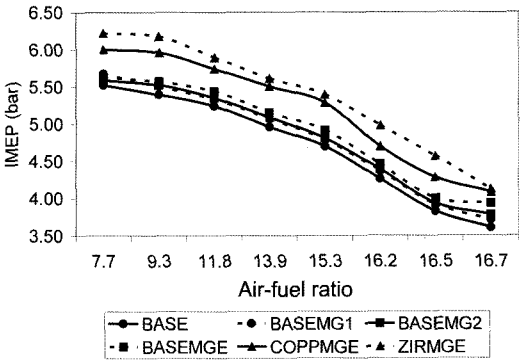

Figure 17. Variation of indicated mean effective pressure with air-fuel ratio.

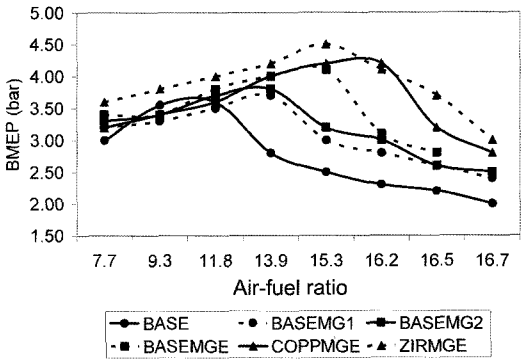

Figure 18. Variation of break mean effective pressure with air-fuel ratio.

varied from the minimum to a maximum extent and graphs drawn for various cylinder parameters versus AFR. Improvement in thermal efficiency and reduction in exhaust emissions mainly depends on magnetic energizing. With an increase of the load on the engine, combustion chamber temperature and air movement increases. To some extent, efficiency increases as the engine is made leaner; then it fails due to the lean misfire

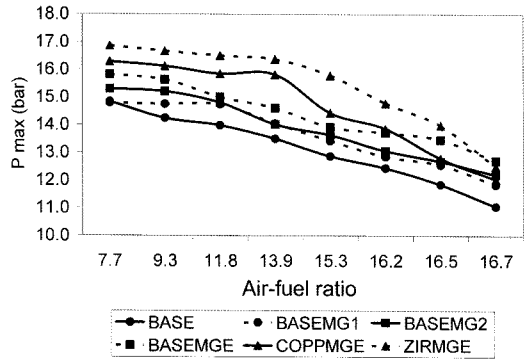

Figure 19. Variation of peak pressure with air-fuel ratio.

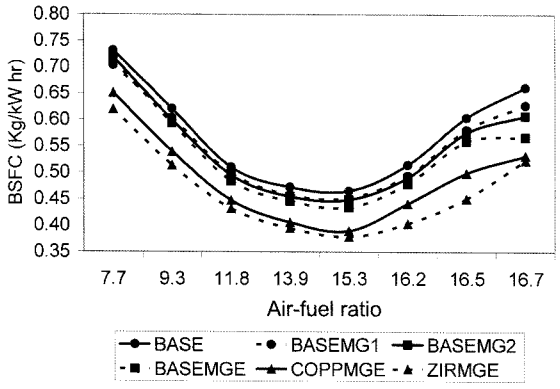

Figure 20. Variation of brake-specific fuel consumption with air-fuel ratio.

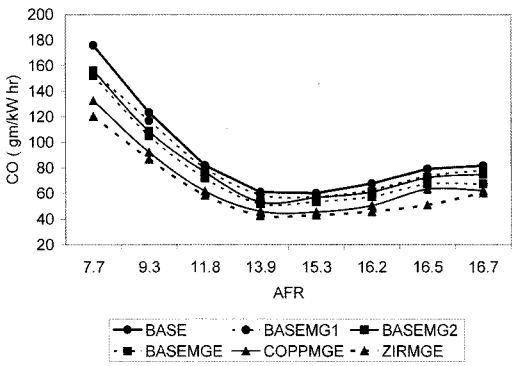

Figure 21. Variation of carbon monoxide with air-fuel ratio.

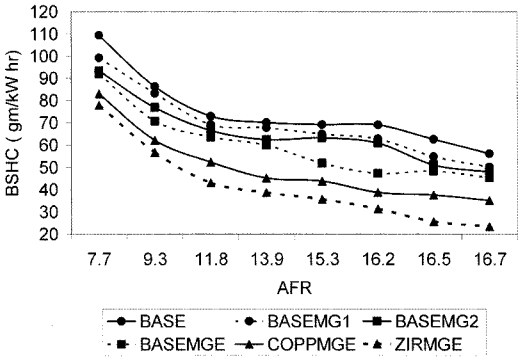

Figure 22. Variation of hydrocarbon with air-fuel ratio.

limit.

6.2. Effect on Cycle Variation

The widely used parameter to analyze the combustion variation in SI engines is peak pressure (P_{max}), as measured inside the cylinder during combustion. As the combustion rate increases due to the energized fuel, the gas force developed by combustion of the charge inside the energized fuel combustion is found to be more than that developed at the base combustion (Janczak *et al.*, 1992). This increased gas force leads to higher peak pressure for the same supply of air-fuel mixture (16.7:1) in an energized fuel engine. Also, cyclic variations in peak pressures are controlled because the combustion rate depends on the diffusion rate of the fuel, which further varies with crank angle position. So, maximum pressure is developed more or less at a constant crank position in a cycle. Thus, the peak pressure at different cycles is improved.

Figures 23 and 24 show scatter-plots of P_{max} and IMEP for individual cycles for both base and energized fuel engines at an optimal air-fuel ratio of 16.7:1. The P_{max} is directly obtained from the measured cylinder pressure trace. The crank angle speed is measured by an optical crank angle encoder. The mean values of these parameters are also indicated in the figures.

P_{max} is a measure of the rate of pressure rise due to combustion. If the combustion is faster, a higher-pressure-rise rate occurs and a higher P_{max} results. The magnitude of the variation depends on whether the combustion is faster or slower. A faster combustion produces a higher Pmax (Soltau, 1961). Also, the P_{max} tends to occur closer to the TDC, whereas a slower burning cycle has a lower Pmax further away from the TDC.

The IMEP is a measure of the work output from the combustion products. A faster pressure rise and a quicker combustion may result in a higher work output. A higher trapped charge may also lead to an increased work output. Hence, the IMEP fluctuations may be due to variation in combustion rate or variation in the quantity of energy released (Sztenderowicz and Heywood, 1990).

It is interesting to note that the variation in P_{max} among these operating modes is higher at the lean side in a catalytic-coated head engine. Similarly, the variation in IMEP is greater in the lean operation. The coefficient of variation (COV) of Pmax and the IMEP are calculated from the cycles belonging to different modes, and then

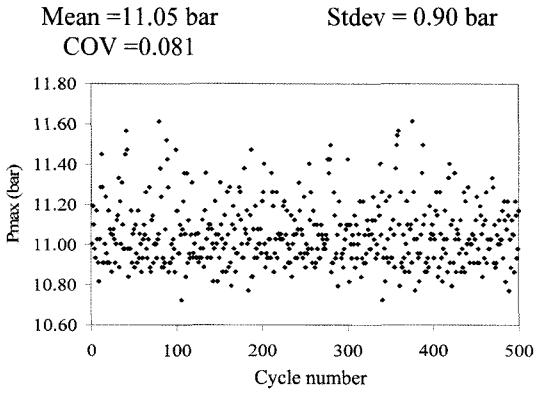

Figure No.? Base engine with absence of magnet

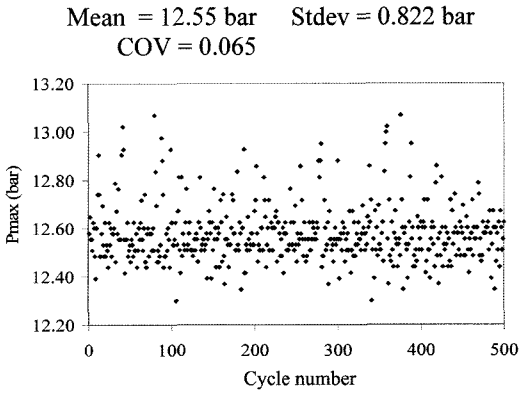

Figure No.? Base Engine with 9000 gauss magnet

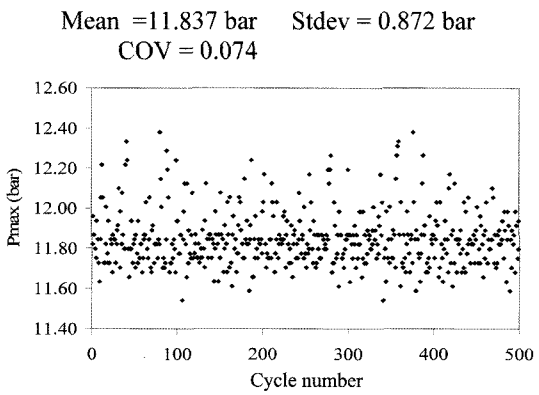

Base Engine with 3000 gauss magnet

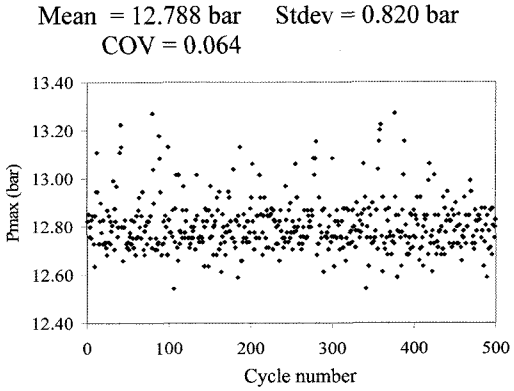

Copper coated Engine with 9000 gauss magnet

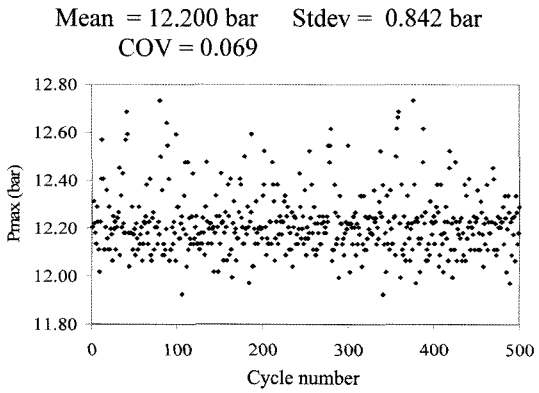

Base Engine with 4500 gauss magnet

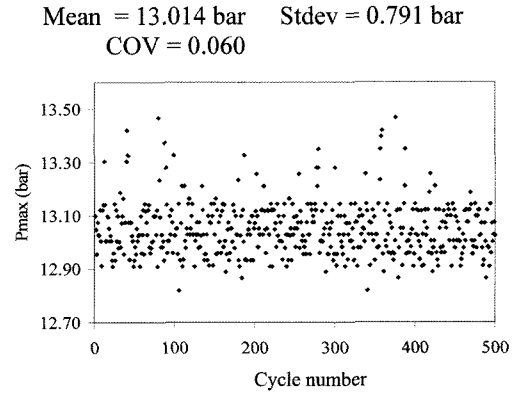

Zirconia coated Engine with 9000 gauss magnet

Figure 23. Scatter plot of peak pressure for different phases of operation at 3000 rpm at an AFR of 16.7

plotted. The COV of Pmax decreases from the base engine to the catalytic-coated head engine, whereas the COV of the IMEP increases.

7. CONCLUSIONS

Brake thermal efficiency and peak pressure significantly increase, while the CO, HC and cyclic variation decrease, in the case of copper- and zirconia-coated engines as compared to a base engine (Table 2).

The variation in peak pressures for continuous cycles of the coated engine (9000 gauss) is less than that of the base engine.

Among the various combinations at the leaner side (AFR=16.7), the zirconia-coated engine with 9000- gauss-magnetic flux has a higher IMEP (4.05 bar) and a lower

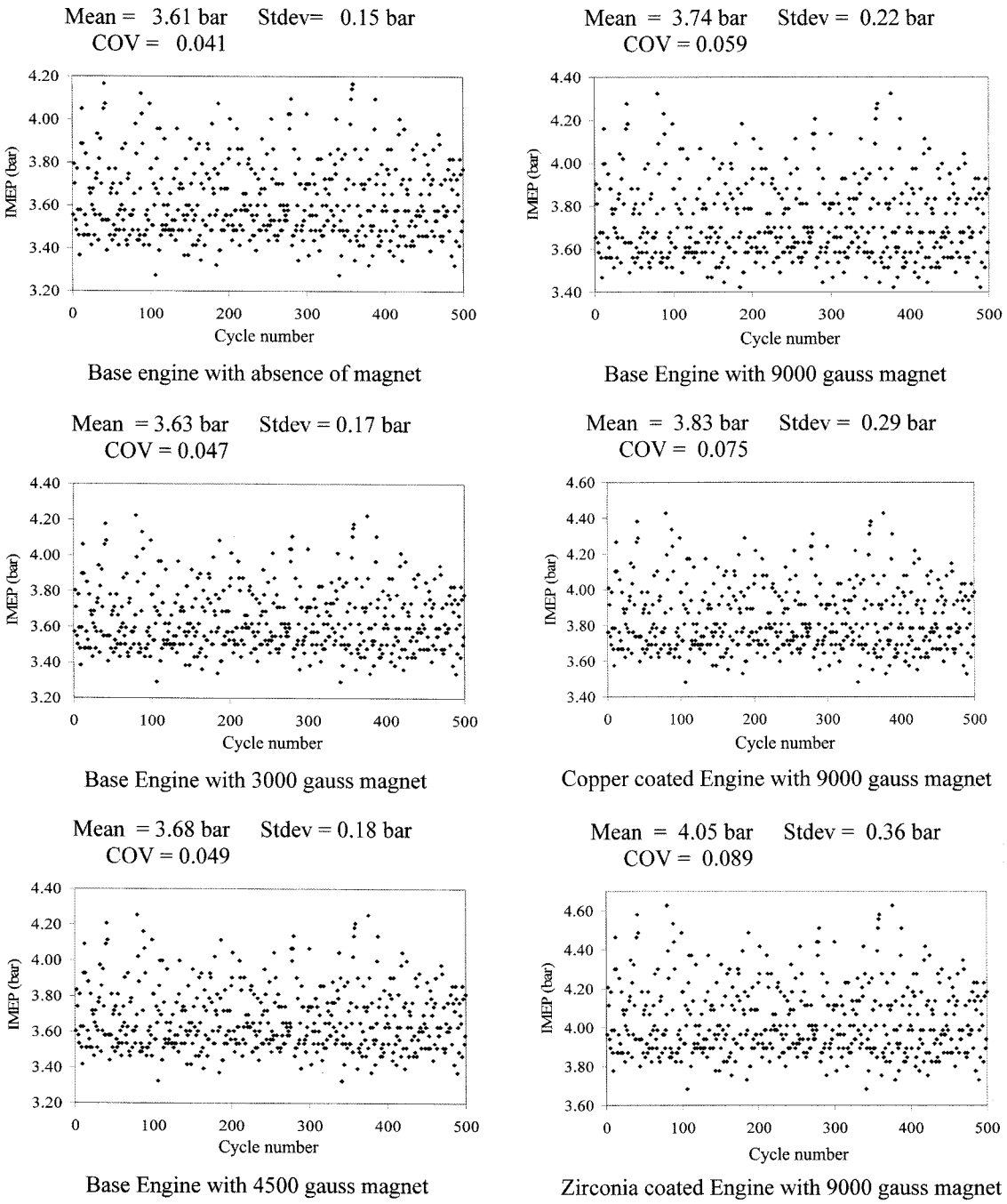

Figure 24. Scatter plot of IMEP for different phases of operation at 3000 rpm at an AFR of 16.7

Table 2. Changes in different parameters with base, Copper- and zirconia-coated engines with 9000 gauss magnetic flux.

Sl. No.	Parameters	Base engine %	Coppercoated engine %	Zirconiacoated engine %
1	Increase in brake thermal efficiency	3.2	6.6	11.2
2	Increase in peak pressure	13.5	15.72	17.78
3	Reduction in cyclic variation	8.6	8.8	12.1
4	Reduction in CO emission	13.3	23.5	29.5
5	Reduction in HC emission	22.1	37.3	44.2

cyclic variation (0.791 bar).

ACKNOWLEDGEMENT–The authors express their sincere thanks to the Department of Science & Technology, Govenment of India for funding the project on Development of Catalytic Activated Lean Burn Combustion.

REFERENCES

Assanis, D., Kevin, Wiese, Emest, Schwarz and Walter, B. (1991). The effects of ceramic coatings on diesel engine performance and exhaust emissions. *SAE Paper No.* 910466.

Dhandapani, S. (1991). *Theoretical and Experimental Investigation of Catalytically Activated Lean Burn Combustion.* Ph. D. Dissertation. IIT Madras. India.

Gao, Z. and Schreiber, W. (2002). A theoretical investigation of two possible modifications to reduce pollutants emissions from a diesel engine. *I Mech E Proc.*, 619.

Hamai, K., Kawajiri, H., Ishizuka, T. and Nakai, M. (1989). Combustion fluctuation mechanism involving cycle-to-cycle spark ignition variation due to flow in SI engines. *21st Symp. (Int.) Combustion*, 312–320.

Heywood, J. B. (1989). *Internal Combustion Engines-Fundamental.* The MIT Press. Cambridge. MA, USA.

Ishibe, N. and Ohira, T. (1995). Combustion analysis and us optimization in two-stroke engines. *SAE Paper No.* 951788.

Janczak, A. and Krensel, E. (1992). *Permanent Magnetic Power for Treating Fuel Lines for Nore Efficient Combustion and Less Pollution.* US Pat 5,124,045.

Kalghahgi, G. T. (1986). Early flame development in a spark ignition engine. *Combustion and Flame*, **60**, 299–308.

Kantor, J. C. (1984). A dynamic instability of spark ignited engine. *Science,* **224**, 1233.

Karim, G. A. (1967). An experimentation of the nature of the random cyclic pressure variations in a spark-ignition engine. *J. Institute of Petroleum,* **53**, 519.

Keek, J. C. and Heywood, J. B. (1987). Early flame development and burning rates in spark ignition engines and their cyclic variability. *SAE Paper No.* 870163.

Kronenberg, K. J. (1985). Experimental evidence for effects of magnetic fields on moving water and fuels. *IEEE Trans. Magnetics*, **21**, 2059–2061.

Marshall, S. V. and Skitek, G. G. (1987). *Electromagnetic Concepts and Applications.* 2nd edn. Englewood Cliffs. Prentice-Hall. New Jersey.

Martin, J. K., Plee, S. L. and Romboski, Jr. D. J. (1988). Burn modes and prior-cycle effects on cyclic variation in lean burn spark ignition combustion. *SAE Paper No.* 88020.

Matekunas, F. A. (1983). Modes and measures of cyclic combustion variability. *SAE Paper No.* 830337.

Mcneely, M. (1994). Magnetic fuel treatment system designed to attack fuel-borne microbes. *Diesel Progress Engines and Drives*, **16**, 107–112.

Nakagawa, Y., Nakai, M. and Hamai, K. (1982). A study of the relationship between cycle-to-cycle variation of combustion and heat release delay in a SI engine. *Bulletin of the JSME* **25**, **199**, 54–60.

Nedunchezhian, N. and Dhandapani, S. (1999). Experimental investigation of cyclic variation of combustion parameters in a catalytically activated two stroke SI engine combustion chamber. *SAE Paper No.* 990014.

Ozdor, N., Dulger, M. and Sher, E. (1994). Cyclic variability in spark ignited engines. A Literature Survey'. *SAE Paper No.* 940987.

Patterson, D. J. (1966). Cylinder pressure variations, a fundamental combustion problem. *SAE Paper No.* 660129.

Peters, B. D. and Borman, G. L. (1970). Cyclic variations and average burning rates in a SI engine. *SAE Paper No.* 700064.

Samuel, S., Austin, L. and Morrey, D. (2002). Automotive test drive cycles for emission measured and real-world emission levels. *I Mech E Proc.*, 555.

Soltau, J. P. (1961). Cylinder pressure variations in petrol engines. *Proc. Inst. Mech. Engrs.*, **2**, 246.

Sztenderowicz, M. L. and Heywood, J. P. (1990). Cycle-to-cycle IMEP fluctuations in stoichiometrically-Fueled SI engine at low speed and load. *SAE Paper No.* 902143.

Tretyakov, I. G., Rybak, M. A. and Stepanenko, E. Y. (1985). Method of monitoring the effectiveness of magnetic treatment for liquid hydrocarbons. *Sov. Surf. Eng. Appl. Electrochem*, **6**, 80–83.

Tsuchiya, K., Nagai, Y. and Gotoh, T. (1983). A study of irregular combustion in a two-stroke cycle gasoline engines. *SAE Paper No.* 830091.

Whitelaw, J. H. and Xu, H. M. (1995). Cyclic variations in a lean-burn spark ignition engine without and with swirl. *SAE Paper No.* 950683.